Colloids and Surfaces B: Biointerfaces 208 (2021) 112047

Contents lists available at ScienceDirect

Colloids and Surfaces B: Biointerfaces

journal homepage: www.elsevier.com/locate/colsurfb

Self-assembly of an aptamer-decorated chimeric peptide nanocarrier for targeted cancer gene delivery

Sadegh Dehghani [a], Mona Alibolandi [b,c], Zeinab Amiri Tehranizadeh [d], Reza Kazemi Oskuee [e], Rahim Nosrati [c,f], Fatemeh Soltani [g,**], Mohammad Ramezani [b,c,*]

[a] Department of Medical Biotechnology and Nanotechnology, Faculty of Medicine, Mashhad University of Medical Sciences, Mashhad, Iran
[b] Pharmaceutical Research Center, Pharmaceutical Technology Institute, Mashhad University of Medical Sciences, Mashhad, Iran
[c] Department of Pharmaceutical Biotechnology, School of Pharmacy, Mashhad University of Medical Sciences, Mashhad, Iran
[d] Department of Medicinal Chemistry, School of Pharmacy, Mashhad University of Medical Sciences, Mashhad, Iran
[e] Targeted Drug Delivery Research Center, Institute of Pharmaceutical Technology, Mashhad University of Medical Sciences, Mashhad, Iran
[f] Cellular and Molecular Research Center, School of Medicine, Guilan University of Medical Sciences, Rasht, Iran
[g] Biotechnology Research Center, Pharmaceutical Technology Institute, Mashhad University of Medical Sciences, Mashhad, Iran

ARTICLE INFO

Keywords:
Non-viral carrier
AS1411 aptamer
Gene delivery
Low molecular weight protamine
Gene transfection

ABSTRACT

In this study, we developed a peptide-based non-viral carrier decorated with aptamer to overcome the specific gene delivery barriers. The carrier (KLN/Apt) was designed to contain multiple functional segments, including 1) two tandem repeating units of low molecular weight protamine (LMWP) to condense DNA into stable nanosize particles and protect it from enzymatic digestion, 2) AS1411 aptamer as targeting moiety to target nucleolin and promote carrier internalization, 3) a synthetic pH-sensitive fusogenic peptide (KALA) for disrupting endosomal membranes and enhancing cytosol escape of the nanoparticles, and 4) a nuclear localization signal (NLS) for active cytoplasmic trafficking and nuclear delivery of DNA. The obtained results revealed the developed carrier capacity in terms of specific cell targeting, overcoming cellular gene delivery barriers, and mediating efficient gene transfection. The KLN/pDNA/aptamer nanoparticles offer remarkable potential for the conceptual design and formation of promising multi-functionalized carriers towards the most demanding therapeutic applications.

1. Introduction

Gene therapy, as a powerful tool, holds tremendous potentials for the treatment of a wide variety of diseases [1]. Thus, to be feasible and viable in a clinical setting, establishing safe, reliable, and efficient delivery carriers is imperative [2,3]. Generally, to efficiently deliver a therapeutic gene to their target sites, the carrier has to overcome different extracellular and cellular barriers including nonspecific protein binding, nuclease degradation, target site transportation, cellular internalization, endosomal entrapment, intracellular cargo release, and its subsequent nuclear transfer (in case of plasmid DNAs) [4–7].

Although viral-based gene carriers account for the majority of gene therapy clinical trials owing to their better transduction efficiency and long-term expression, yet the high immunogenicity, limited packaging capacity, insertional mutagenesis risk, possible carcinogenicity, poor tissue target-specificity and difficulty of large-scale production limit their future applications [4,8,9]. On the contrary, non-viral counterparts have become promising alternates to viral carriers in the last few decades due to their low host immunogenicity, biocompatibility with different biological systems, larger genetic payload capacity, ease of synthesis, modification, and scale-up [4,10,11].

Recently, cationic lipids, liposomes, cationic polymers, dendrimers, graphene, chitosan, and so on, have been investigated as non-viral gene delivery vehicles to overcome some of gene delivery barriers. Although each class of these non-viral carriers has its advantages, lower transfection efficiency and transient gene expression and higher cytotoxicity than virus-derived vectors are some critical issues all still needed to be solved [4,10,12–14].

Peptide-based nanocarriers have attracted intensive research interests in recent years and demonstrated great potential compared to other non-viral delivery systems owing to their unique structure and properties, including their biocompatibility and biodegradability *in vivo*,

* Corresponding author at: School of Pharmacy, Pharmaceutical Research Center, Mashhad University of Medical Sciences, Mashhad, Iran.
** Corresponding author.
E-mail addresses: soltanif@mums.ac.ir (F. Soltani), ramezanim@mums.ac.ir (M. Ramezani).

https://doi.org/10.1016/j.colsurfb.2021.112047
Received 15 December 2020; Received in revised form 17 July 2021; Accepted 14 August 2021
Available online 16 August 2021

limited/no toxicity, the amphipathic or cationic structure, chemical diversity, and stability in a wide range of biological conditions [5, 15–17]. Genetic engineering techniques allow us to rationally design multi-functional peptide-based virus-mimicking nanocarriers containing multiple natural and, or synthetic domains [18]. Using this approach, a genetically engineered chimeric peptide as a gene carrier with a programmed amino acid sequence and well-recognized relationship between structure, sequence, length, and gene transfer efficiency of the carrier at the molecular and nano-scale levels could be prepared to bypass the barriers of the gene delivery [18,19].

Low molecular weight protamine (LMWP) is a natural arginine-rich peptide obtained from the enzymatic digestion of protamine. Previous studies reported that LMWP enhanced intracellular delivery of therapeutic nucleic acids and proteins, drug-conjugated polymers, and nanoparticles [20,21]. Also, LMWP has a safe, non-toxic, and non-immunogenic profile. Therefore, LMWP can be practically applied as an efficient and safe cationic peptide for condensing DNA and improving intracellular cargo delivery [20,22,23].

In the present study, we designed an aptamer-functionalized multivalent peptide-based biomimetic nanocarrier with several critical functional properties for safe and efficient gene delivery. In this system, we incorporated two tandem repeating units of LMWP (L) to condense the plasmid DNA (pDNA) into nanosize particles through electrostatic self-assembly, improving protection from nuclease degradation, a synthetic fusogenic peptide named KALA for pH-triggered destabilization of the endosomal membrane (K), and a monopartite simian virus 40 (SV40) large T-antigen NLS (N) to mediate the cytosol trafficking and nuclear transportation of pDNA. Besides, due to the promising abilities of aptamers as targeting moieties [24], AS1411 aptamer (Apt), an approved anti nucleolin aptamer [25], was used to target model cells and enhance selective targeting and endocytic uptake of the carrier system. For simplicity, the carrier will be shown as KLN/Apt (Fig. 1). LMWP is the key fragment of the designed carrier and was investigated for the first time in conjunction with fusogenic and nuclear localizing motifs in a chimeric architecture. In this experiment, we will describe the design and recombinant expression of the engineered single-chain recombinant peptide nanocarrier and each segment functionality in the carrier structure regarding effective pDNA condensation, cellular targetability, pH-dependent endosome membrane-disruptive activity, and mediating cytoplasmic trafficking, as well as active nuclear entry would be investigated using a series of *in vitro* assays.

2. Materials and methods

2.1. Bioinformatic study

Amino acid sequences of multiple candidate chimeric peptides were designed based on different motif arrangements. The threading approach using the online I-TASEER servers [26] was used to model the three-dimensional (3D) structures of the chimeric peptides. Next, the modeled structures were evaluated using SAVES servers [27] in terms of solvent accessibility, atomic environment, and stereochemistry. The best models were introduced to NPDOCK software to investigate the possible interactions with a template B-DNA (PDB ID: 1BNA). Finally, the best docking results in the case of docking score and conformation were selected for further evaluations.

2.2. Biosynthesis of the recombinant chimeric peptide

The gene encoding KALA-2LMWP-NLS (KLN) peptide, inserted into

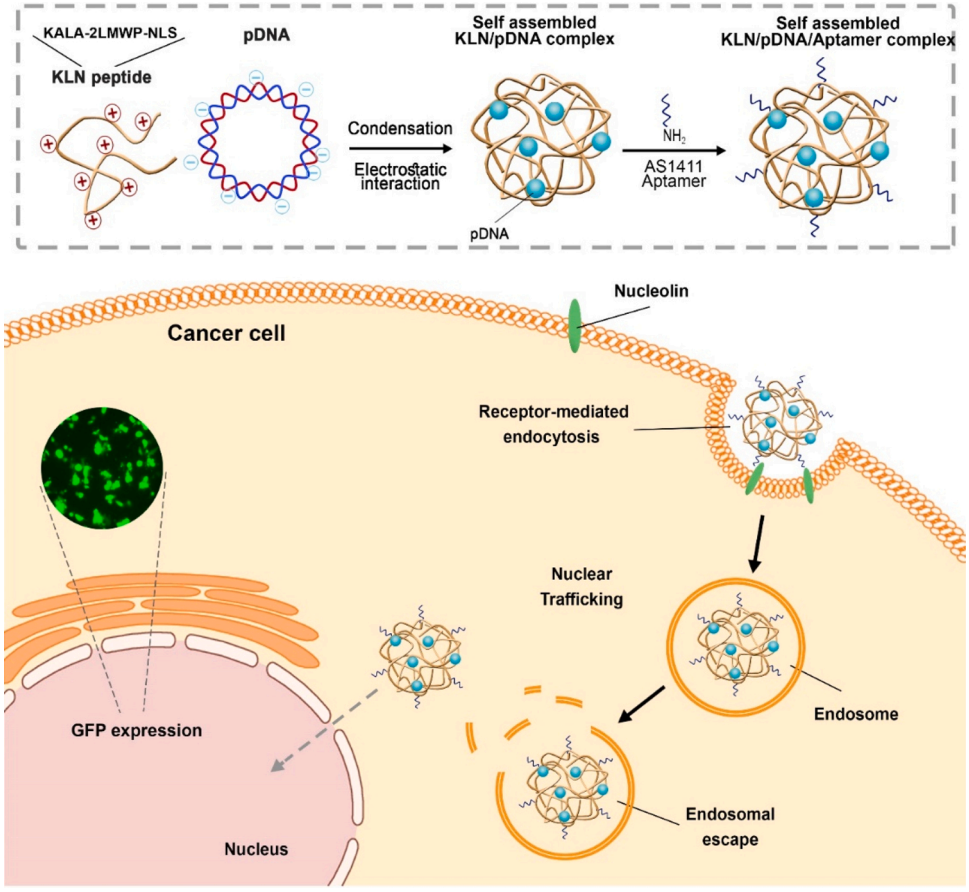

Fig. 1. Schematic representation of KLN/pDNA/Aptamer formulation as a gene delivery vector and its fate until reaching into the nucleus. K: KALA; L: low molecular weight protamine; N: NLS.

the NdeI/Xho1 restriction sites, was designed and codon-optimized. In the next step, the gene was synthesized and subcloned into the pET21b expression plasmid at the NdeI and Xho1 positions of its multiple cloning sites, containing a T7 promoter by Biomatik company (Canada). The amino acid sequences for each motif of the KLN is as follows: KALA: WEAKLAKALAKALAKHLAKALAKALKASEA; LMWP: VSRRRRRRGG RRRR; NLS: KPKKKRKV

The constructed recombinant plasmid was then transformed into the *Escherichia coli* strain BL21 (DE3) as expression host. The resulting positive clone was grown at 37 °C in 2-YT medium containing 100 μg/mL ampicillin. Then final working concentration of 0.5 mM isopropyl β-D-1-thiogalactopyranoside (IPTG) was added into the growth medium at an OD600 of 0.6 to induce the over-expression of the KLN at 30 °C. Next, the KLN was purified from bacterial pellets following nickel-chelate affinity chromatography (Ni-NTA). Bacterial cells were harvested by centrifugation for 10 min at 6000 × g at 4 °C, and pellets were resuspended and homogenized in lysis buffer containing 50 mM NaH_2PO_4, 500 mM NaCl, 8 M urea, 0.5 % Triton X-100, 10 mM imidazole (pH 8.0) to disrupt the bacterial cell walls. Then, the insoluble debris were removed by centrifugation at 12,000 × *g* (30 min, 4 °C). The solubilized fraction was added to 1 mL pre-equilibrated Ni-NTA agarose (Qiagen) and incubated for 1 h at room temperature with mild shaking. After sufficient binding has occurred, the resin was loaded into an empty nickel column, pre-equilibrated with lysis buffer (20 mL), unbound peptides initially were removed by washing with 30 mL wash buffer containing 50 mM NaH_2PO_4, 1000 mM NaCl, 20 mM imidazole, 7 M urea, 0.5 % Triton X-100 (pH 8.0), and the KLN was then eluted with 5 mL elution buffer containing 50 mM NaH_2PO_4, 200 mM NaCl, 250 mM imidazole, 5 M urea (pH 8.0). Finally, Western blot analysis and SDS-PAGE were applied to investigate the expression and purity of the target peptide, respectively.

2.3. Desalting and preparation of peptide stock solution

An *in vitro* sequential dialysis with a gradual reduction of urea concentration was performed to refold the denatured purified peptide [28]. To decrease the chance of salt bridge formation between particles and subsequent aggregation which affects nanoparticle size and to remove the excess ions interfering with the electrostatic interactions of the peptide sequence and pDNA, a desalting step was performed. Desalting and buffer exchange of the purified peptide was performed by dialysis membrane Spectra/Por (3 kDa MWCO) against acetate buffer (5 mM, 200 mM NaCl, pH 5.5) at 4 °C for 4 h and then acetate buffer (5 mM, 50 mM NaCl, pH 5.5) overnight. Amicon ultracentrifugal filter unit (5 KD MWCO 15 mL, Millipore) was used to concentrate the dialyzed solution, and a stock solution of 0.5 mg/mL was stored at −20 °C (200 μL aliquots), avoiding freeze/thaw cycles.

2.4. KLN/pDNA/aptamer complex formation

Electrophoretic mobility shift assay (EMSA) or gel retardation assay was performed to investigate the negative charge neutralization and complexation of pDNA by the KLN and aptamer binding to KLN/pDNA (pMAXGFP) polyplexes. KLN/pDNA polyplexes were prepared with different N/P ratios (nitrogen to phosphate ratio) of 0–22. Briefly, increasing amounts of KLN in equal volumes were mixed with a constant concentration of pDNA (1 μg) and vortexed for 15 s. Next, the mixtures were incubated at room temperature for 20 min to allow the formation of polyplexes and then added to wells of agarose gel (1 %, pre-stained with GelRed®). Gel electrophoresis was performed in Tris–acetate-EDTA buffer (1 %) at 80 V for 20 min.

For the preparation of KLN/pDNA/aptamer complexes, AS1411 aptamer, having a sequence of 5′ GGTGGTGGTGGTTGTGG TGGTGGTGG-3′ at final concentrations of 1, 2, and 5 μM, was directly added to different N/P ratios of KLN/pDNA polyplexes, in which pDNA was efficiently condensed and retarded, followed by a room temperature incubation for 15 min. The electrostatic binding of different aptamer concentrations to KLN/pDNA polyplexes was confirmed by a 2.5 % gel retardation assay. Moreover, a 1 % agarose gel electrophoresis with a KLN/pDNA/aptamer complex was also performed. The volumes of all formulations were also kept constant during the complexes preparation.

2.5. Characterization of complexes

The particle sizes, zeta potentials, and polydispersity index (PDI) of the KLN/pDNA polyplexes and KLN/pDNA/aptamer complexes were determined using dynamic light scattering (DLS) method (Malvern Zetasizer Nano ZS unit Instrument, UK) at 25 °C. At the time of measurement, the solution was diluted with 5 mM acetate buffer, pH 5.5 to a total volume of 1 mL.

The particle size and morphology of complexes were also characterized using scanning electron microscopy (SEM) analysis at N/P of 16. Briefly, a solution of complex was deposited and dried on a metal stub at room temperature, and a thin gold layer was sputtered on the surface. A field emission scanning electron microscope (FESEM, TESCAN, Czech Republic) was applied to capture the corresponding images of nanoparticle. The measurements were carried out in automatic mode.

2.6. Serum stability analysis

To investigate serum stability, in the first group, KLN/pDNA and KLN/pDNA/aptamer complexes at the N/P ratio of 16 were prepared as mentioned above. In the next group, 10 % (v/v) non-heat-inactivated fetal bovine serum (FBS) was added to prepare stable complexes, and incubation was allowed to stand for 30 min (37 °C). In the last group, to dissociate pDNA and aptamer from the complexes, 10 % SDS was added after 30 min of incubation with serum at 37 °C. To confirm the effectiveness of serum nuclease activity, the naked pDNA and aptamer, incubated with serum (10 % v/v), were used as controls. The released pDNA and aptamer were electrophoresed and visually examined on 1 % and 2.5 % agarose gel, respectively.

2.7. Hemolysis assay

The membrane-disruptive activity of the KLN was measured using a red blood cell (RBC) hemolysis assay. Human RBCs were collected after whole blood centrifugation at 800 × g for 10 min at 4 °C, and the plasma was aspirated and discarded. After washing the RBCs with PBS twice, the pellet of RBCs was diluted in PBS (pH 7.4) or acetate buffer (50 mM, pH 5.5), and NaCl was used to adjust for physiological-like ionic strength. Then, the diluted RBCs solutions (100 μL, 2×10^8 cells) were added to 1, 5, 10, and 20 μg of the KLN peptide. After incubation (37 °C for 60 min) and centrifugation of the solutions at 300 × g for 15 min, a microplate reader was used to measure the supernatant absorbance values at 405 nm (BioTeK, USA). PBS and Triton X-100 (1 % v/v) treated RBCs, were employed as controls for 0 % and 100 % hemolysis, respectively.

2.8. Cell-cycle synchronization

To synchronize MCF-7 cells in the G1 status, cells were cultured in a 24-well plate at a density of 7×10^4 cells/well in RPMI 1640 with 10 % FBS and incubated overnight in a humidified incubator (37 °C and 5 % CO_2). After 24 h, cell-cycle synchronization was carried out by replacing the culture medium with fresh hydroxyurea-containing medium (2.5 mM) and incubation of the cells for 18 h. Next, the synchronized cells were used for the transfection study.

2.9. Cell transfection studies

For measurement of transfection efficiency and to confirm the cell-selective transfection, MCF-7 (cell surface nucleolin positive) and MCF-10A (cell surface nucleolin negative) breast cancer cells were

seeded in RPMI 1640 containing 10 % FBS and DMEM/F12 supplemented with horse serum (5 %), respectively, at a density of 7×10^4 cells/well in a 24-well plate and cultures were incubated at 37 °C before transfection. The KLN/pDNA and KLN/pDNA/aptamer complexes at different N/P ratios (8, 12, 16, and 20) were prepared in PBS (pH 7.4) at a final solution volume of 150 μL. When cells reached approximately 80 % confluency, the medium was aspirated and discarded, and 150 μL of complexes diluted in 150 μL serum-free medium and medium containing 10 % FBS, was added to each well. After incubation for 4 h at 37 °C, the transfection mixture was removed followed by adding fresh serum-containing medium and incubation for 36 h to allow the expression of green fluorescent protein (GFP). Transfection assays with chloroquine (100 μM, Sigma-Aldrich) were also conducted by adding chloroquine to the cells 45 min before transfection.

To visualize cells expressing GFP, the plates were observed by JuLI™ Smart fluorescent cell viewer (NanoEnTek, Korea Republic). After that, the cells were rinsed with PBS, detached by trypsin, and centrifuged for 5 min at 400 × g. The supernatant was discarded and the cell pellets were rinsed twice with 300 μL of cold PBS, and GFP-positive cells were quantified *via* flow cytometry (BD FACSCalibur™). Data analysis was performed using FlowJo software. Each time, 10,000 cells were counted. Naked pDNA (1 μg pMAXGFP) and PEI (branched 25 kDa) were as the negative and positive controls, respectively.

2.10. Inhibition study

To investigate the role of nucleolin in the enhancement of the transfection efficiency, nucleolin positive MCF-7 cells were seeded in 24-well plates and incubated with AS1411 aptamer at various concentrations (5, 10, and 20 μM) for 30 min followed by adding the KLN/pDNA/aptamer complexes at N/P ratio of 16. After incubation at 37 °C for 4 h, the medium was replaced with a fresh medium supplemented with 10 % FBS. The cells were detached 36 after transfection, washed with PBS as described above, and GFP-positive cells were quantified *via* flow cytometry. Untreated cells were the controls while transfected with KLN/pDNA/aptamer complexes (N/P ratio of 16).

2.11. Measurement of cytotoxicity

MCF-7 and MCF-10A cells, at a density of 1×10^4 cells/well, were seeded into 96-well culture plates. The medium was replaced with a fresh serum-free medium after incubating for 24 h, and 100 μL solutions of prepared complexes at different N/P ratios were added to each well. After incubation at 37 °C for 4 h, the medium was aspirated and replaced with fresh complete medium containing serum, and the plates were incubated for the next 36 h. Untreated cells and PEI 25 kDa were used as negative and positive controls, respectively. Afterward, MTT stock solution (20 μL, 5 mg/mL) was added to each well, and after 4 h of incubation, the cell supernatant was completely aspirated. For dissolving of formazan crystals, DMSO (100 μL/well) was added, and the absorbances were determined by a microplate reader (BioTeK, USA) at 570 nm wavelength. Then, the percent of cell viability relative to untreated cells, was measured after normalizing wavelength values with the absorbance of untreated cells.

2.12. Statistical analysis

Statistical assessment was conducted by *t*-test. All results were obtained from three independent measurements and reported as mean ± standard deviation (SD) ($n = 3$). All statistical analyses were conducted using Graphpad Prism software. $P < 0.05$ was considered statistically significant.

3. Results and discussion

3.1. The modeled structure of the recombinant chimeric peptide

Initial investigations on tertiary structures showed that repeated LMWP sequences more than twice destroyed both the tertiary protein structure and the level of structural compaction. Among the predicted structures, several models were selected to evaluate their interactions with DNA. Based on the protein-nucleic acid docking results obtained from NPDOCK software [29], KALA-2LMWP-NLS was selected as the best candidate for expression. In this structure, KALA and LMWP helixes were separated with a flexible intermediate-length linker, which made an eligible structure in secondary and tertiary structures. According to the analysis, the model created from this sequence is ideal and flawless, indicating the correct positioning of the flexible loops. Finally, regarding the functions predicted for each domain previously, the maximum interactions between the LMWP sequence and the DNA strands were observed, which were mainly electrostatic (data not shown).

3.2. Recombinant production and purification of the chimeric peptide

Following in silico studies and selection of the best chimeric peptide candidate, the gene encoding chimeric peptide was constructed and subcloned into the pET21b expression plasmid with C-terminal 6x-His-tag and T7 promoter locations. DNA sequencing verified the sequence of the gene with no signs of mutation or deletion. The KLN was expressed in *E. coli* Bl21 (DE3) as inclusion bodies after evaluating different induction times, temperatures, and IPTG concentrations. Optimum expression of the KLN was obtained with 0.5 mM IPTG at 30 °C for 8 h (Supplementary Fig. 1). Western blotting using a mouse monoclonal antibody against the C-terminal His-tag confirmed the expression of the recombinant peptide. After Ni-NTA purification of the expressed peptide, the purity of the peptide was confirmed by SDS-PAGE 15 % (Supplementary Fig. 2), and a production yield of about 1 mg purified peptide per 1 L growth culture was obtained.

Despite the calculated molecular weight (MW) of the KLN (10,787 Da), an approximately 14 kD single band was found higher than the anticipated MW. This distinct increase in MW is associated with the high positive charge density on the peptide due to multiple arginine and lysine residues, leading to the insufficiency of charge neutralization by SDS and partially retarded peptide movement. Some other studies have reported similar observations [30].

3.3. Complex formation and protection by the KLN

The crucial role of a cationic peptide as a non-viral gene delivery carrier is to produce stable nanosize particles with negatively charged deoxyribonucleic acid by electrostatic force-induced self-assembly [3]. Based on the results of our *in silico* studies, we incorporated two tandem repeating units of LMWP within the amino acid primary structure of KLN and evaluated its complexation capability. The prepared KLN/pDNA polyplexes determined the point where uncharged polyplexes were formed, signified by the retention of pDNA in the loading wells. As shown in Fig. 2A, pDNA was condensed efficiently at N/P ratios higher than 8 on 1 % gel agarose.

Based on this result, KLN/pDNA polyplexes at different N/P ratios of 8, 12, 16, and 20 were chosen for examining the aptamer binding. The results revealed that aptamer at concentrations of 1 and 2 μM were attached entirely to all polyplexes, but this was not observed at 5 μM of aptamer, as shown in 2.5 % gel agarose (Fig. 2B). Then, the 2 μM concentration was selected for subsequent experiments. Moreover, the result of electrophoresis on 1 % agarose gel showed that binding of the aptamer to KLN/pDNA polyplexes did not affect the integrity of the KLN/pDNA polyplexes and KLN/pDNA/aptamer complexes remained intact and contained all three components (Fig. 2C).

Sufficient biostability, especially protection from serum nucleases

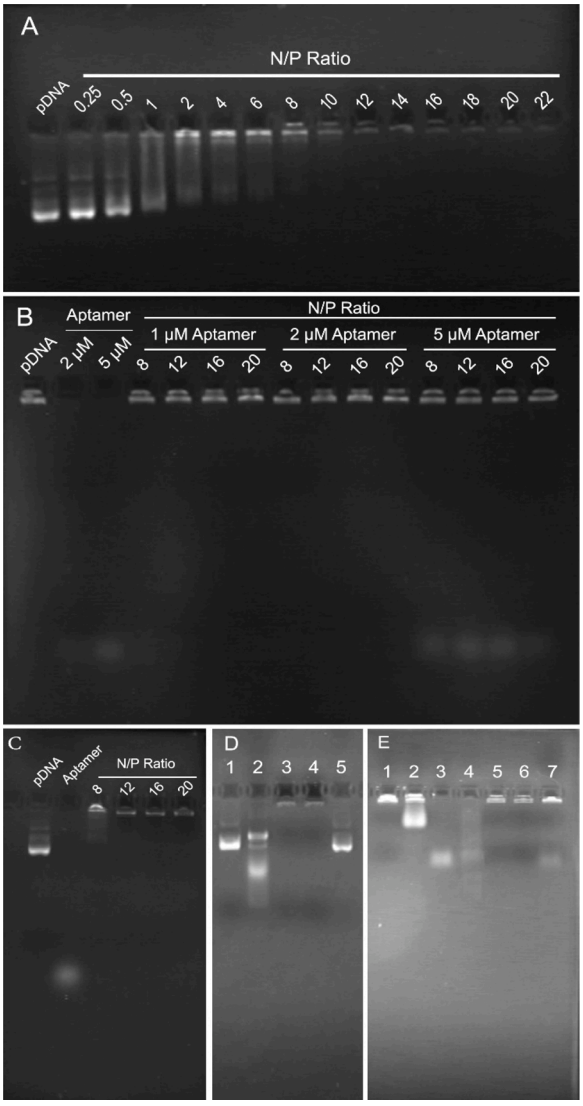

Fig. 2. (A–C): Complex formation assay. A) Gel mobility pattern of KLN/pDNA polyplexes at N/P ratios of 0.25 to 22. Naked pDNA corresponds to N/P ratio of 0 (1 % gel agarose). B) Gel mobility pattern of KLN/pDNA/aptamer complexes at N/P ratios of 8 to 20 (2.5 % gel agarose). C) Gel mobility pattern of KLN/pDNA/aptamer complexes at N/P ratios of 8 to 20 (1 % gel agarose). D) Serum stability of KLN/pDNA polyplexes (N/P ratio of 16, 1 % gel agarose). Lane 1: naked pDNA without serum. Lane 2: serum-incubated naked pDNA. Lane 3: KLN/pDNA polyplexes without serum. Lane 4: serum-incubated KLN/pDNA polyplexes. Lane 5: recovered pDNA from the KLN/pDNA polyplexes after 10 % serum and SDS incubation. E) Serum stability of KLN/pDNA/aptamer complexes (N/P ratio of 16, 2.5 % gel agarose). Lane 1: naked pDNA without serum. Lane 2: serum-incubated naked pDNA. Lane 3: AS1411 aptamer without serum. Lane 4: serum-incubated AS1411 aptamer. Lane 5: KLN/pDNA/aptamer complexes without serum. Lane 6: serum-incubated KLN/pDNA/aptamer complexes. Lane 7: recovered AS1411 aptamer from the KLN/pDNA/aptamer complexes after 10 % serum and SDS incubation.

digestion, is a fundamental feature of potential nanocarriers for gene delivery applications [31]. The serum stability of the complexes and pDNA and aptamer protection from nuclease activity was also well-studied. Given the results, the pDNA and aptamer in the complexes showed stability upon treatment with 10 % FBS. At the same time, naked pDNA and aptamer were degraded following serum treatment and the recovered pDNA and aptamer remained intact after SDS treatment (Fig. 2D&E). These results suggested that KLN could not only condense pDNA but also protect it together with aptamer from serum endonuclease cleavage, which could contribute to the potential application of this gene delivery system.

3.4. Characterization of the physical properties of polyplexes

For targeted nanoparticles, the surface potentials, particle sizes, and morphology are critical factors that govern the cellular entry and affect the gene transfer efficiency [2]. The morphology and particle properties of KLN/pDNA and KLN/pDNA/aptamer complexes at different N/P ratios (8, 12, 16, and 20) were investigated. As illustrated in Fig. 3A, at 8–20 N/P ratios, the pDNA was completely condensed into KLN/pDNA polyplexes with a maximum size limit of 200 nm suitable for clathrin-mediated endocytosis [5,18]. Furthermore, the value of zeta potential increased with an increase in N/P ratios, indicating the full complexation of pDNA by KLN (Fig. 3A). Moreover, by adding a constant concentration of aptamer to each complex, with increasing the N/P ratios, a slight increase in size was observed and, net surface charge of KLN/pDNA/aptamer complexes decreased moderately, still positive zeta potentials were observed at all N/P ratios. PDI of KLN/pDNA/aptamer complexes was around 0.3, as shown in Fig. 3B. The observed PDI values higher than 0.3 may be due to formation of some aggregates before and during formulation process which could be further optimized. Overall, changes in size and surface charge of KLN/pDNA polyplexes may indicate that more of the added aptamer probably is localized onto the surface of the polyplexes.

The SEM analysis of KLN/pDNA and KLN/pDNA/aptamer complexes confirmed size measurements by DLS and showed that KLN peptide condensed pDNA and formed compact KLN/pDNA (Fig. 3C) and KLN/pDNA/aptamer (Fig. 3D) complexes with spherical morphologies.

3.5. Hemolytic activity of KLN

As the N-terminal fragment of the KLN structure, a pH-sensitive membrane destabilizing peptide (KALA) is located to enhance the transport of pDNA from the endosome to the cytoplasm. Therefore, to investigate the specific endosomolytic activity of fusogenic peptide KALA and determine that this activity was maintained when KALA was integrated into KLN, an RBC hemolysis assay at both extracellular and endosomal pH values (7.4 and 5.5 respectively) was performed. This characteristic of KALA is essential as the membrane disruption should be limited to endosomal vesicles in a pH-dependent procedure, preventing nonspecific membrane damage [32].

The KLN peptide revealed no membrane-disruptive functionality at physiological conditions (pH 7.4), similar to the negative control (PBS buffer) ($p > 0.05$). On the other hand, the hemolytic activity of KLN peptide significantly increased at acidic pH 5.5 compared to the negative control in a concentration-dependent manner, indicating that hemolytic activity of the KLN is dependent on both pH and concentration (Fig. 4). Based on the hemolysis assay, the fusogenic activity of KALA is preserved at the N-terminus of KLN.

3.6. Transfection study

To further study the gene transfer capability of the carrier, the transfection of plasmid GFP mediated by this gene delivery system was carried out in the absence and presence of 10 % serum and the percentage of live cells expressing the GFP gene was utilized to assess the efficiency of transfection. Transfection of MCF-7 and MCF-10A cells was performed using with various N/P ratios of the KLN/pDNA and KLN/pDNA/aptamer complexes to determine the optimal transfection ratio. According to the results, in the absence of serum, the general trend of transfection study with KLN/pDNA/aptamer complexes showed efficient gene transfer at all tested N/P ratios in MCF-7 cells. The highest degree of transfection efficiency (30.9 % of cells) was obtained at N/P ratio of 16, which was adopted in the following experiments (Fig. 5A). In order to provide a better prediction of the performance of the designed formulation for *in vivo* studies and to evaluate the effect of serum on the

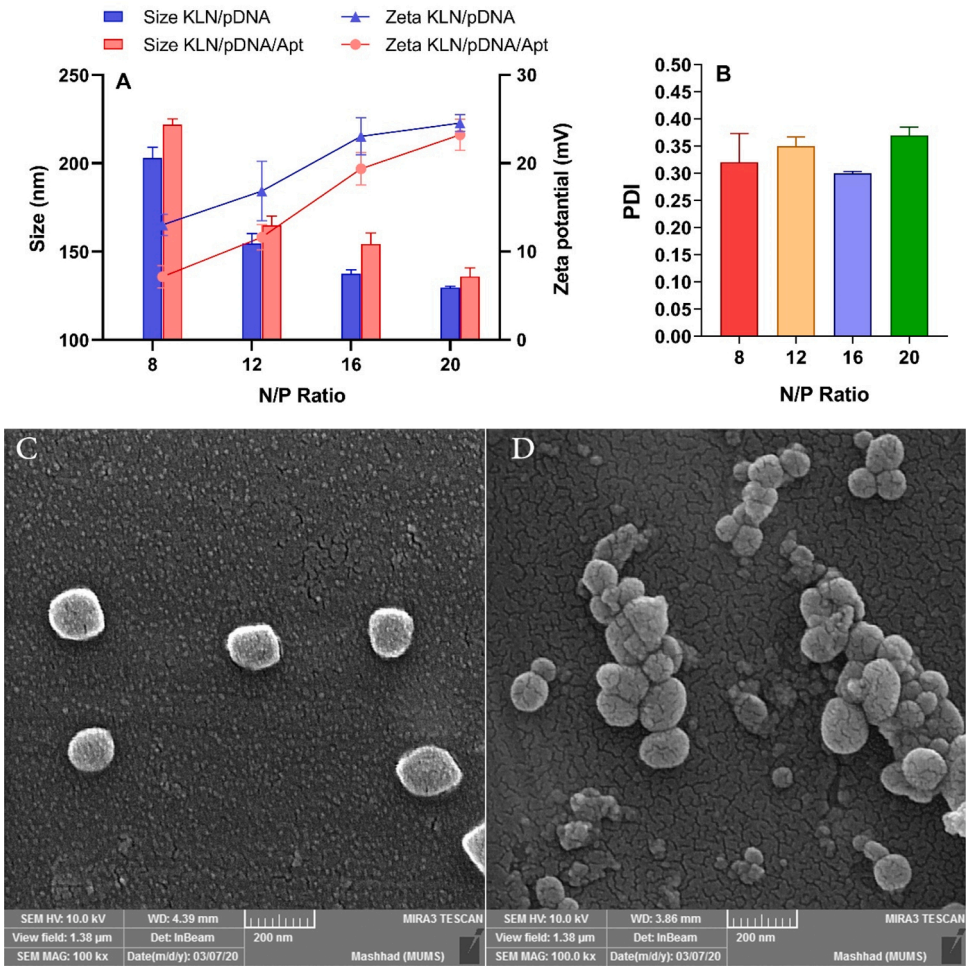

Fig. 3. Characterization of designed delivery system. A) The particle size and charge distribution analysis of KLN/pDNA and KLN/pDNA/aptamer complexes at different N/P ratios by using dynamic light scattering. B) PDI of KLN/pDNA/aptamer complexes at various N/P ratios. SEM images of complexes prepared with KLN/pDNA (C) and KLN/pDNA/aptamer (D) at N/P ratio of 16. Data are presented as mean ± SD, n = 3.

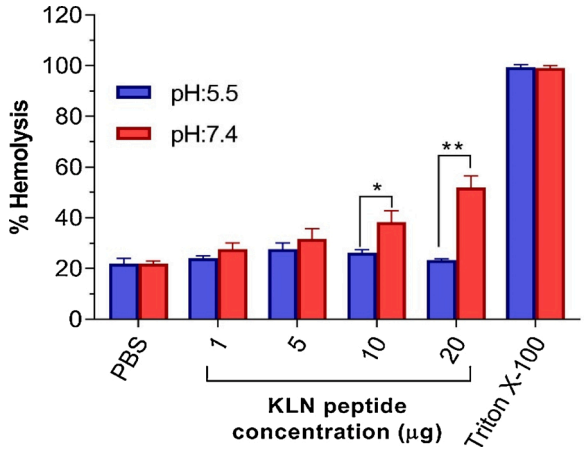

Fig. 4. Hemolysis assay for KLN at two pH (*i.e.*, 7.4 and 5.5) and various concentrations. PBS buffer and Triton X-100 were used as negative and positive controls, respectively. The data is reported as mean ± SD, n = 3.

transfection efficiency, transfection assay was also performed in the presence of 10 % serum. The transfection efficiency of the KLN/pDNA/aptamer complexes was reduced in the presence of serum, at all tested N/P ratios (Fig. 5B). In the meantime, no detectable GFP expression was observed for cells transfected with naked pDNA in the absence and presence of serum (Fig. 5A&B).

As a positive control, we used branched PEI 25 KD to validate the transfection protocol. In comparison with KLN/pDNA/aptamer complexes, a higher rate of gene transfer for PEI was observed in the absence and presence of serum (Fig. 5A&B) that is likely due to the increased cationic charge density upon complex formation, enabling interaction of PEI/pDNA complex with the negatively charged components on the membrane. However, severe *in vivo* toxicity of PEI could be due to its strong cationic density and its inherent non-degradability [33,34]. Similar to KLN/pDNA/aptamer complexes, presence of serum reduced the transfection efficiency of the PEI/pDNA complexes at all tested N/P ratios (Fig. 5B). Reduction in transfection efficiency of KLN/pDNA/aptamer and PEI/pDNA particles could be attributed to competitive binding of serum proteins to the positively charged complexes through non-specific electrostatic interactions, leading to lower cellular uptake. Generally, decreasing the surface positive charge of complexes by chemical modification may solve this problem. The percentages of GFP positive cells in the absence and presence of 10 % serum at N/P of 16 are indicated as flow cytometry histogram plots in Fig. 5C.

3.7. Evaluation of functionality of AS1411 aptamer

It has been demonstrated that active targeting with nanocarrier decorated with a targeting moiety that recognizes receptors overexpressed or uniquely expressed on the target cancer cells *versus* normal cells, greatly improved their target cell-internalization [18,35]. In the

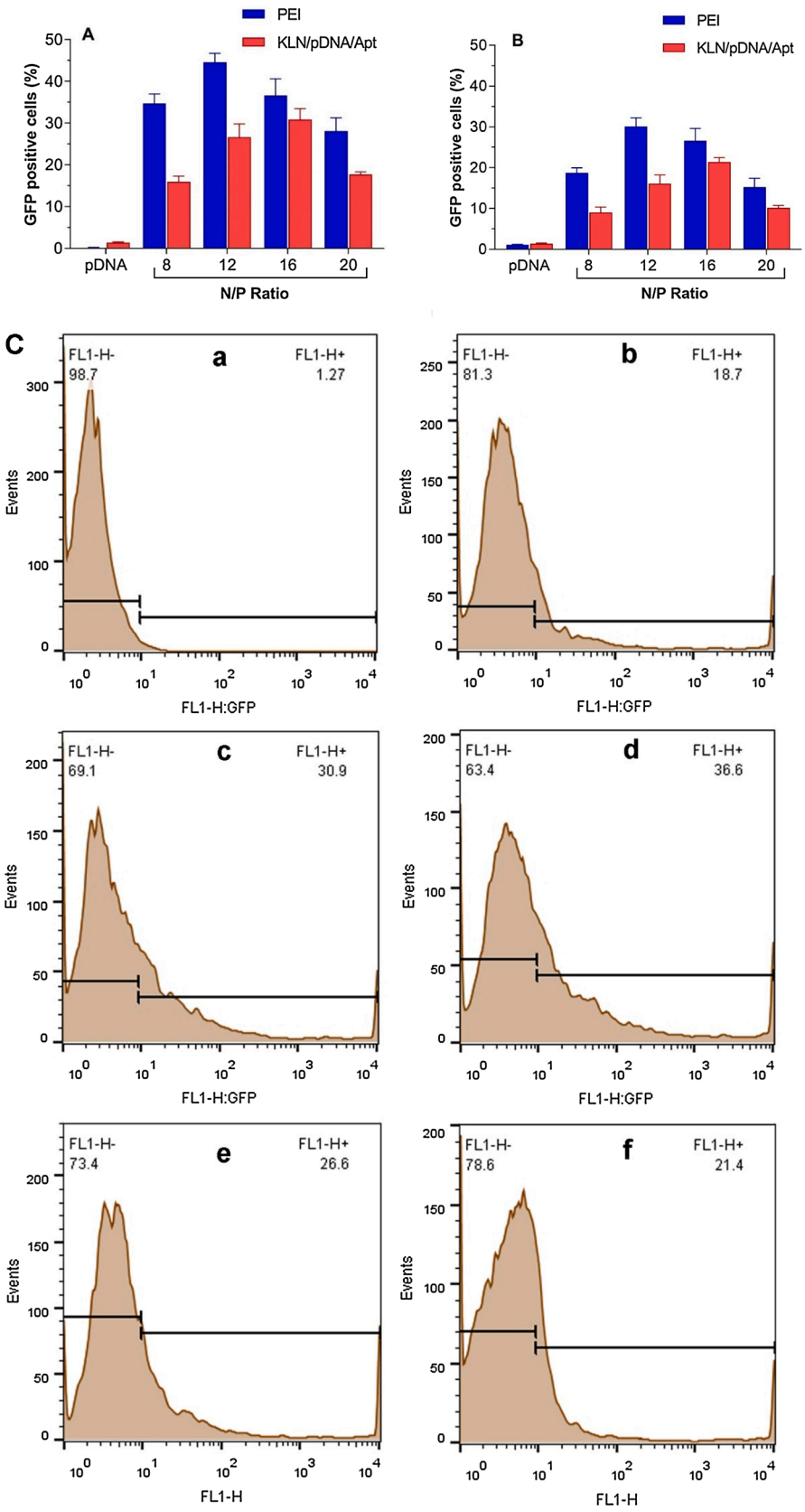

Fig. 5. Gene transfection efficiency. A) Percent of GFP positive MCF-7 cells transfected with KLN/pDNA/aptamer and PEI/pDNA complexes at different N/P ratios in the absence of serum. B) Percent of GFP positive MCF-7 cells transfected with KLN/pDNA/aptamer and PEI/pDNA complexes at different N/P ratios in the presence of 10 % serum. The percentage of transfected cells is measured by flow cytometer. C) Flow cytometry histograms representing the percent of GFP positive MCF-7 cells transfected with naked pDNA in the absence of serum (a), KLN/pDNA polyplex at N/P of 16 in the absence of serum (b), KLN/pDNA/aptamer complex at N/P of 16 in the absence of serum (c), PEI/pDNA polyplex at N/P of 16 in the absence of serum (d), KLN/pDNA/aptamer complex at N/P of 16 in the presence of serum (e), and PEI/pDNA polyplex at N/P of 16 in the presence of serum (f).

present study, an AS1411 aptamer with a high affinity towards cell surface nucleolin was included in the carrier structure. Considering that AS1411 was the first aptamer in clinical trials for cancer treatment and currently is in phase II of clinical trials, AS1411-functionalized nanoparticles could be used for targeted gene and drug delivery because of high surface expression of nucleolin on the surface of several cancer cell lines [36]. *In vitro* and *in vivo* results of different investigations indicated that both covalently and non-covalently conjugation of AS1411 to various types of nanoparticles or other platforms is an ideal strategy for enhancing subsequent uptake of these cargoes by the cancer cells [25, 36–42]. Considering the fact that compact structures of aptamers with extensive double-stranded content, make aptamers potentially resistant to conformation change, we expected in our non-covalent strategy, despite its simplicity and convenient preparation, nucleolin-binding site of AS1411 aptamer, electrostatically attached to KLN/pDNA polyplexes, is expose on the surface of the complexes, ensuring highly specific recognition by the overexpressed nucleolin on the cancer cells, thereby leading to the enhancement of transfection efficiency.

To further confirm the aptamer functionality in the complexes and to investigate the nucleolin-mediated internalization of KLN/pDNA/aptamer complexes into the cells, we carried out an inhibition experiment. Based on the results, the reduction in the efficient internalization of complexes and of gene expression levels confirmed that the cellular entry of complexes was *via* nucleolin (Fig. 6A). These results are consistent with previous observations that the interaction of AS1411 aptamer and nucleolin, induced receptor-mediated endocytosis [43,44].

Furthermore, to examine the targeted and cell-selective delivery of the nanoparticles, MCF-7 and MCF-10A cell lines were transfected as model cells. Wu et al. [41] have previously demonstrated that the AS1411-modified nanoparticle can selectively target MCF-7 cancer cells over-expressing nucleolin. As a negative control, we chose the MCF-10A cell as a non-cancerous cell line that does not over-express nucleolin [41]. The higher number of transfected MCF-7 cells compared to significantly lower number of MCF-10A cells after incubation with KLN/pDNA/aptamer complexes, might be explained by cell-surface levels of nucleolin. Besides, the absence of aptamer in the complexes led to the reduction in transfection efficiency in MCF-7 cells without an obvious difference in the transfection efficiency of KLN/pDNA and KLN/pDNA/aptamer complexes in MCF-10A cells. Moreover, no significant change in transfection efficiency was observed between MCF-7 and MCF-10A cells transfected with KLN/pDNA complexes (Fig. 6B). These findings demonstrated that a functional AS1411 aptamer in the complexes improved the entry of particles into the nucleolin positive cells thereby significantly enhanced the GFP expression. Additionally, because of the cell-penetrating activities of LMWP [21,22], the observed transfection efficiency of KLN/pDNA complexes might be due to the presence of LMWP in the structure of KLN peptide. Furthermore, both cell lines were transfected with PEI with a relatively high level of efficiency in a non-selective manner (Fig. 6B).

3.8. Assessment of KALA and NLS functionality

To elucidate the membrane-destabilizing activity of KALA in the KLN structure, and to evaluate the endosomal escape activity of internalized nanoparticles, we measured the transfection efficiency of KLN/pDNA/aptamer complexes at two N/P ratios of 12 and 16 in the presence of

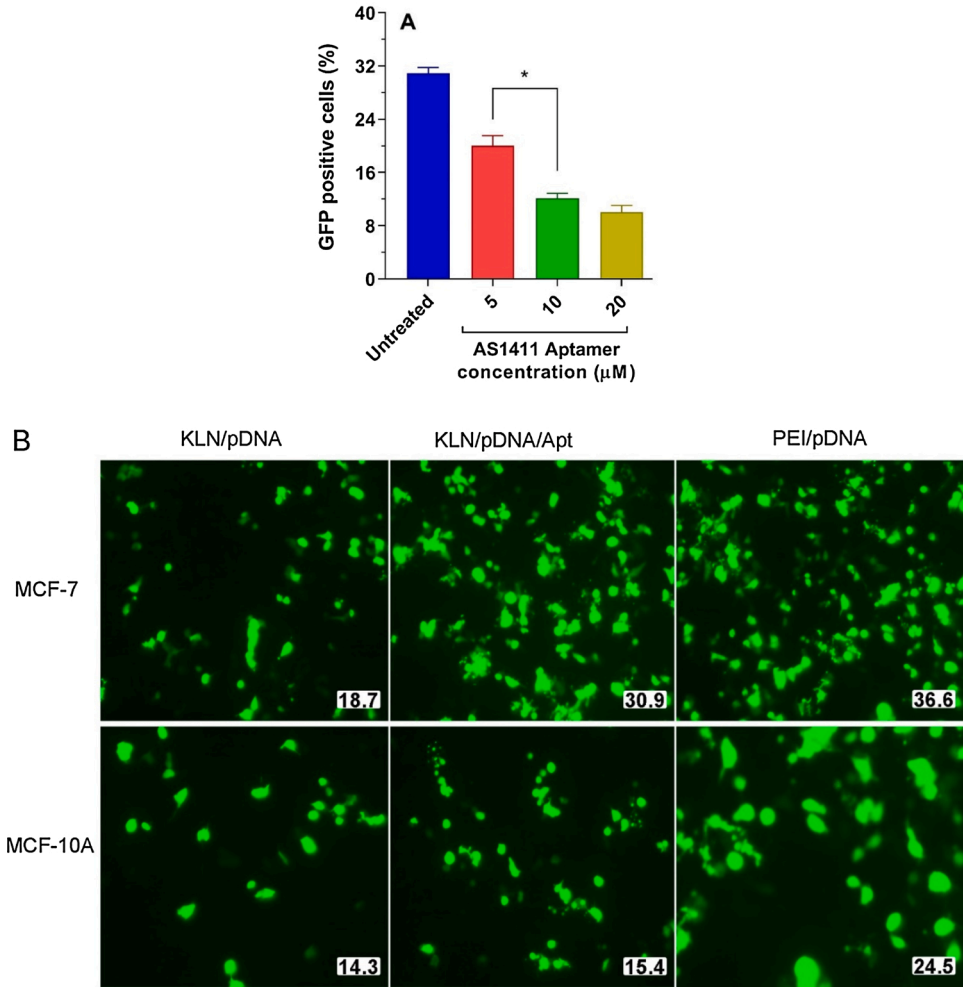

Fig. 6. Validation of nucleolin targeted gene transfer. A) In an inhibition assay, cells were pretreated with aptamer to validate the complexes' internalization into the cells through nucleolin-dependent endocytosis. Different concentrations of aptamer (competitive inhibitor) were used. The results are reported as mean ± SD, n = 3. B) Qualitative representation of MCF-7 and MCF-10A cells transfected with KLN/pDNA and KLN/pDNA/aptamer complexes at N/P ratio of 16. PEI/pDNA complexes were used as a positive control. The percentage of GFP positive cells is determined by flow cytometer.

chloroquine. Chloroquine, a lysosomotropic compound, promotes endosomal disruption and facilitates the cytoplasmic release of the cargo [5,45]. Interestingly, the transfection efficiency of the polyplexes in the presence of chloroquine did not significantly change, implying that the majority of the internalized complexes escaped from the endosomal entrapment without the help of chloroquine (Fig. 7A). These results were consistent and confirmed the findings observed in hemolysis assay and indicated that complexes could successfully escape the endosome as a result of the pH-responsive activity of KALA, thereby mediating efficient GFP expression. Moreover, the endosomal membranes rupture can be associated with the proton sponge effect of His-tag in the KLN structure [18,35].

After efficient endosomal escape, the condensed pDNA should be transferred efficiently into the nucleus, where the pDNA is released for gene expression to occur [18]. The presence of an NLS which can mediate the transport of cargoes to the nucleus through nuclear pore complexes could be the key to overcome this problem. Generally, in cells undergoing division during mitosis, the nuclear membrane starts disappearing, and pDNA can reach the nucleus. In contrast, in non-dividing cells, the nuclear delivery of pDNA requires the use of an NLS, which could minimize nuclear pore complex (NPC)-independent nuclear transport [7,46]. To examine the functionality of NLS in the KLN structure, and to evaluate whether the nuclear delivery of pDNA was promoted *via* NPC, MCF-7 cells were synchronized using hydroxyurea, a cell cycle inhibitor at the G1 phase [7]. Meanwhile, GFP expression in transfected cells with PEI/pDNA at N/P ratios of 12 and 16 as controls was dramatically reduced when hydroxyurea inhibited mitosis ($p < 0.05$). On the contrary, the transfection efficiencies with KLN/pDNA/aptamer complexes at N/P ratios of 12 and 16 showed that transgene expression was inhibited slightly ($p > 0.05$) in non-dividing cells compared to that of dividing cells (Fig. 7B). These results demonstrated that the treatment with hydroxyurea restricted the process of NPC-independent nuclear transfer, and nuclear localization of pDNA in synchronized cells could be associated with the presence of functional NLS in the KLN structure. Overall, these findings demonstrated that NLS-containing carriers can promote the process of nuclear delivery.

3.9. Cell viability assay

To assess the cytotoxicity of KLN/pDNA/aptamer complexes and its possible effect on cell transfection efficiency, MCF-7 and MCF-10A cells were incubated with the complexes. As illustrated in Fig. 8A, no significant toxicity was observed in MCF-7 cells at all N/P ratios compared to that of negative control (pDNA only). As cancer cells behave differently from normal cells, a cell viability experiment may not give a similar toxicity outcome on normal cells. The same trend observed for normal MCF-10A cells compared to cancer cells at all N/P ratios (Fig. 8B). Overall, the cell viabilities of both cell lines treated with different N/P ratios of KLN/pDNA/aptamer complexes were more than 80 %. Different studies showed that the formation of PEI/pDNA complex may reduce the cytotoxicity of PEI unlike its high cytotoxic activity in non-complexed form. Consistent with previous studies, in our cell viability experiment, PEI/pDNA complexes showed slight ($p > 0.05$) cytotoxicity in comparison with KLN/pDNA/aptamer complexes. However, the cytotoxicity of PEI is not acceptable for clinical application. The obtained cytotoxicity of PEI/pDNA complexes may be associated with a higher positive surface charge of the PEI/pDNA complexes, destabilizing the cell membrane by interacting with several negatively-charged proteins. Overall, the KLN/pDNA/aptamer complexes can be utilized safely due to negligible cytotoxicity in both cancer and normal cells. This low cytotoxicity of KLN-based complexes could lead to higher transfection efficiency.

4. Conclusion

In the current work, we developed a multi-functional gene delivery carrier with chimeric architecture, preserving the individual functionality of the incorporated segments. The KLN peptide showed excellent pDNA complexation capacity, appreciable gene protection capability against enzymatic degradation, and blood compatibility with negligible hemolysis under a physiological environment. The complexation of the KLN with GFP plasmid and AS1411 aptamer is multifaceted. It formed spherical nanoparticles with acceptable size and surface charge properties, remarkably enhanced the targeted cellular internalization *via* receptor-mediated endocytosis, showed an effective endosomal escape, and enhanced nuclear transfer of genetic material leading to superior transfection efficiency. In addition to this, the nanoparticles indicated negligible cytotoxicity in both cancer and normal cells. The ternary nano-platform developed in the present study offers a promising gene delivery system towards the evaluation of its further therapeutic and animal studies.

CRediT authorship contribution statement

Sadegh Dehghani: Conceptualization, Methodology, Writing - original draft. **Mona Alibolandi:** Project administration, Writing - review & editing. **Zeinab Amiri Tehranizadeh:** Methodology, Visualization. **Reza Kazemi Oskuee:** Project administration, Resources. **Rahim Nosrati:** Conceptualization, Writing - original draft. **Fatemeh Soltani:** . **Mohammad Ramezani:** Supervision, Funding acquisition, Project administration.

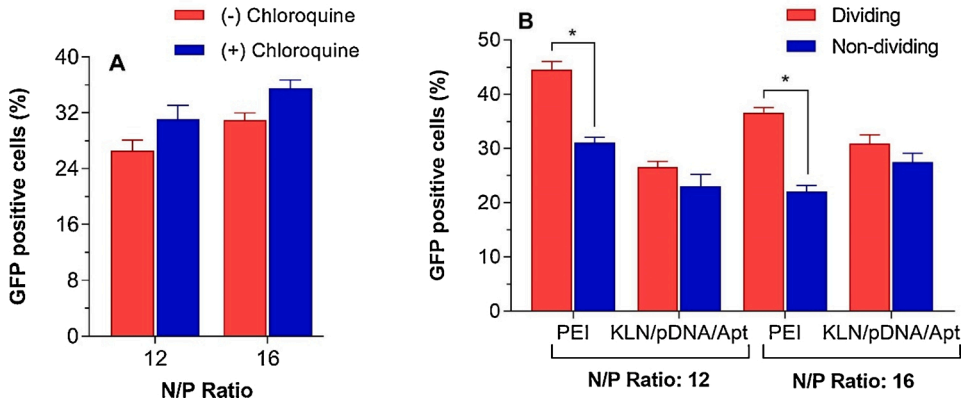

Fig. 7. A) Impact of chloroquine treatment (100 μM) on the transfection efficiency of KLN/pDNA/aptamer complexes at two various N/P ratios. The results are reported as mean ± SD, n = 3. B) Assessment of the nuclear localization signal functionality. Dividing and non-dividing MCF-7 cells were transfected with KLN/pDNA/aptamer and PEI/pDNA complexes at two various N/P ratios. The results are reported as mean ± SD, n = 3.

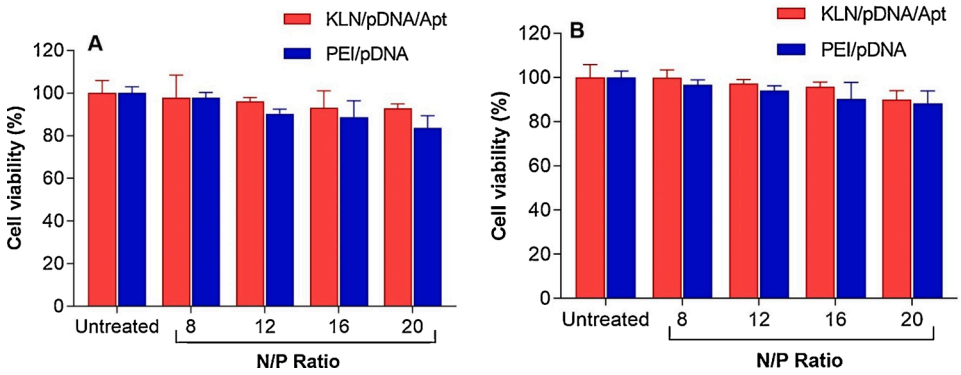

Fig. 8. Corresponding cell viabilities of KLN/pDNA/aptamer and PEI/pDNA complexes in (A) MCF-7 and (B) MCF-10A cells. Data are reported as mean ± SD, n = 3.

Declaration of Competing Interest

The authors report no declarations of interest.

Acknowledgments

The data presented in this report was a part of the Ph.D. thesis (Grant NO. 950722) supported by Mashhad University of Medical Sciences. This study was also financially supported by grant No. 960209 of the Biotechnology Development Council of the Islamic Republic of Iran.

Appendix A. Supplementary data

Supplementary material related to this article can be found, in the online version, at doi:https://doi.org/10.1016/j.colsurfb.2021.112047.

References

[1] A. Kargaard, J.P. Sluijter, B. Klumperman, Polymeric siRNA gene delivery–transfection efficiency versus cytotoxicity, J. Control. Release 316 (2019) 263–291.
[2] Â. Sousa, A.M. Almeida, R. Faria, K. Konate, P. Boisguerin, J.A. Queiroz, D. Costa, Optimization of peptide-plasmid DNA vectors formulation for gene delivery in cancer therapy exploring design of experiments, Colloids Surf. B Biointerfaces 183 (2019), 110417.
[3] H.O. McCarthy, J. McCaffrey, C.M. McCrudden, A. Zholobenko, A.A. Ali, J. W. McBride, A.S. Massey, S. Pentlavalli, K.-H. Chen, G. Cole, Development and characterization of self-assembling nanoparticles using a bio-inspired amphipathic peptide for gene delivery, J. Control. Release 189 (2014) 141–149.
[4] I.A. Khalil, S. Kimura, Y. Sato, H. Harashima, Synergism between a cell penetrating peptide and a pH-sensitive cationic lipid in efficient gene delivery based on double-coated nanoparticles, J. Control. Release 275 (2018) 107–116.
[5] A.A. Begum, Y. Wan, I. Toth, P.M. Moyle, Bombesin/oligoarginine fusion peptides for gastrin releasing peptide receptor (GRPR) targeted gene delivery, Biorg. Med. Chem. 26 (2018) 516–526.
[6] B. Chen, C. Wu, Cationic cell penetrating peptide modified SNARE protein VAMP8 as free chains for gene delivery, Biomater. Sci. 6 (2018) 2647–2655.
[7] H.-Y. Wang, J.-X. Chen, Y.-X. Sun, J.-Z. Deng, C. Li, X.-Z. Zhang, R.-X. Zhuo, Construction of cell penetrating peptide vectors with N-terminal stearylated nuclear localization signal for targeted delivery of DNA into the cell nuclei, J. Control. Release 155 (2011) 26–33.
[8] L. Liu, Z.-M. Zong, Q. Liu, S.-S. Jiang, Q. Zhang, L.-Q. Cen, J. Gao, X.-G. Gao, J.-D. Huang, Y. Liu, A novel galactose-PEG-conjugated biodegradable copolymer is an efficient gene delivery vector for immunotherapy of hepatocellular carcinoma, Biomaterials 184 (2018) 20–30.
[9] S. Yang, C. Ou, L. Wang, X. Liu, J. Yang, X. Wang, M. Wang, M. Shen, Q. Wu, C. Gong, Virus-esque nucleus-targeting nanoparticles deliver trojan plasmid for release of anti-tumor shuttle protein, J. Control. Release 320 (2020) 253–264.
[10] N.A. Alhakamy, P. Dhar, C.J. Berkland, Charge type, charge spacing, and hydrophobicity of arginine-rich cell-penetrating peptides dictate gene transfection, Mol. Pharm. 13 (2016) 1047–1057.
[11] J. Mesken, A. Iltzsche, D. Mulac, K. Langer, Modifying plasmid-loaded HSA-nanoparticles with cell penetrating peptides–cellular uptake and enhanced gene delivery, Int. J. Pharm. 522 (2017) 198–209.
[12] U.R. Dahiya, S. Mishra, S. Chattopadhyay, A. Kumari, A. Gangal, M. Ganguli, Role of cellular retention and intracellular state in controlling gene delivery efficiency of multiple nonviral carriers, ACS Omega 4 (2019) 20547–20557.
[13] R.M. Raftery, D.P. Walsh, L.B. Ferreras, I.M. Castaño, G. Chen, M. LeMoine, G. Osman, K.M. Shakesheff, J.E. Dixon, F.J. O'Brien, Highly versatile cell-penetrating peptide loaded scaffold for efficient and localised gene delivery to multiple cell types: from development to application in tissue engineering, Biomaterials 216 (2019), 119277.
[14] M. Mashal, N. Attia, G. Martínez-Navarrete, C. Soto-Sánchez, E. Fernández, S. Grijalvo, R. Eritja, G. Puras, J.L. Pedraz, Gene delivery to the rat retina by non-viral vectors based on chloroquine-containing cationic niosomes, J. Control. Release 304 (2019) 181–190.
[15] Y. Hu, H. Wang, H. Song, M. Young, Y. Fan, F.-J. Xu, X. Qu, X. Lei, Y. Liu, G. Cheng, Peptide-grafted dextran vectors for efficient and high-loading gene delivery, Biomater. Sci. 7 (2019) 1543–1553.
[16] C. Jeong, J. Yoo, D. Lee, Y.-C. Kim, A branched TAT cell-penetrating peptide as a novel delivery carrier for the efficient gene transfection, Biomater. Res. 20 (2016) 1–8.
[17] K. Konate, M. Dussot, G. Aldrian, A. Vaissière, V. Viguier, I.F. Neira, F. Couillaud, E. Vivès, P. Boisguerin, S. Deshayes, Peptide-based nanoparticles to rapidly and efficiently "Wrap'n roll" siRNA into cells, Bioconjug. Chem. 30 (2018) 592–603.
[18] Y. Wang, S.S. Mangipudi, B.F. Canine, A. Hatefi, A designer biomimetic vector with a chimeric architecture for targeted gene transfer, J. Control. Release 137 (2009) 46.
[19] B.F. Canine, Y. Wang, A. Hatefi, Evaluation of the effect of vector architecture on DNA condensation and gene transfer efficiency, J. Control. Release 129 (2008) 117–123.
[20] H. He, J. Ye, E. Liu, Q. Liang, Q. Liu, V.C. Yang, Low molecular weight protamine (LMWP): a nontoxic protamine substitute and an effective cell-penetrating peptide, J. Control. Release 193 (2014) 63–73.
[21] Y.-S. Choi, J.Y. Lee, J.S. Suh, Y.-M. Kwon, S.-J. Lee, J.-K. Chung, D.-S. Lee, V. C. Yang, C.-P. Chung, Y.-J. Park, The systemic delivery of siRNAs by a cell penetrating peptide, low molecular weight protamine, Biomaterials 31 (2010) 1429–1443.
[22] H. Xia, X. Gao, G. Gu, Z. Liu, N. Zeng, Q. Hu, Q. Song, L. Yao, Z. Pang, X. Jiang, Low molecular weight protamine-functionalized nanoparticles for drug delivery to the brain after intranasal administration, Biomaterials 32 (2011) 9888–9898.
[23] S. Arabzadeh, Z.A. Tehranizadeh, H.M. Haghighi, F. Charbgoo, M. Ramezani, F. Soltani, Design, synthesis, and in vitro evaluation of low molecular weight protamine (LMWP)-based amphiphilic conjugates as gene delivery carriers, AAPS PharmSciTech 20 (2019) 111.
[24] D. Xiang, C. Zheng, S.-F. Zhou, S. Qiao, P.H.-L. Tran, C. Pu, Y. Li, L. Kong, A. Z. Kouzani, J. Lin, Superior performance of aptamer in tumor penetration over antibody: implication of aptamer-based theranostics in solid tumors, Theranostics 5 (2015) 1083.
[25] L. Li, J. Hou, X. Liu, Y. Guo, Y. Wu, L. Zhang, Z. Yang, Nucleolin-targeting liposomes guided by aptamer AS1411 for the delivery of siRNA for the treatment of malignant melanomas, Biomaterials 35 (2014) 3840–3850.
[26] J. Yang, Y. Zhang, I-TASSER server: new development for protein structure and function predictions, Nucleic Acids Res. 43 (2015) W174–W181.
[27] E. Schreiner, L.G. Trabuco, P.L. Freddolino, K. Schulten, Stereochemical errors and their implications for molecular dynamics simulations, BMC Bioinformatics 12 (2011) 1–9.
[28] A. Maleksabet, H. Zarei Jaliani, A. Asgari, A. Ramezani, N. Erfani, Specific targeting of recombinant human pancreatic ribonuclease 1 using gonadotropin-releasing hormone targeting peptide toward gonadotropin-releasing hormone receptor-positive cancer cells, Iran. J. Med. Sci. 46 (4) (2020) 281.
[29] I. Tuszynska, M. Magnus, K. Jonak, W. Dawson, J.M. Bujnicki, NPDock: a web server for protein–nucleic acid docking, Nucleic Acids Res. 43 (2015) W425–W430.
[30] A. Majidi, M. Nikkhah, F. Sadeghian, S. Hosseinkhani, Development of novel recombinant biomimetic chimeric MPG-based peptide as nanocarriers for gene delivery: imitation of a real cargo, Eur. J. Pharm. Biopharm. 107 (2016) 191–204.
[31] Z. Zhou, X. Liu, D. Zhu, Y. Wang, Z. Zhang, X. Zhou, N. Qiu, X. Chen, Y. Shen, Nonviral cancer gene therapy: delivery cascade and vector nanoproperty integration, Adv. Drug Del. Rev. 115 (2017) 115–154.
[32] F.S. Nouri, X. Wang, M. Dorrani, Z. Karjoo, A. Hatefi, A recombinant biopolymeric platform for reliable evaluation of the activity of pH-responsive amphiphile fusogenic peptides, Biomacromolecules 14 (2013) 2033–2040.
[33] Y. Cui, X. Li, K. Zeljic, S. Shan, Z. Qiu, Z. Wang, Effect of PEGylated magnetic PLGA-PEI nanoparticles on primary hippocampal neurons: reduced

nanoneurotoxicity and enhanced transfection efficiency with magnetofection, ACS Appl. Mater. Interfaces 11 (2019) 38190–38204.
[34] C. Jiang, J. Chen, Z. Li, Z. Wang, W. Zhang, J. Liu, Recent advances in the development of polyethylenimine-based gene vectors for safe and efficient gene delivery, Expert Opin. Drug Deliv. 16 (2019) 363–376.
[35] S.S. Mangipudi, B.F. Canine, Y. Wang, A. Hatefi, Development of a genetically engineered biomimetic vector for targeted gene transfer to breast cancer cells, Mol. Pharm. 6 (2009) 1100–1109.
[36] R. Deng, N. Shen, Y. Yang, H. Yu, S. Xu, Y.-W. Yang, S. Liu, K. Meguellati, F. Yan, Targeting epigenetic pathway with gold nanoparticles for acute myeloid leukemia therapy, Biomaterials 167 (2018) 80–90.
[37] C. Xu, X.-Y. He, Y. Peng, B.-S. Dai, B.-Y. Liu, S.-X. Cheng, Facile strategy to enhance specificity and sensitivity of molecular beacons by an aptamer-functionalized delivery vector, Anal. Chem. 92 (2019) 2088–2096.
[38] P.J. Bates, E.M. Reyes-Reyes, M.T. Malik, E.M. Murphy, M.G. O'toole, J.O. Trent, G-quadruplex oligonucleotide AS1411 as a cancer-targeting agent: uses and mechanisms, Biochim. Biophys. Acta Gen. Subj. 1861 (2017) 1414–1428.
[39] J. Carvalho, A. Paiva, M.P.C. Campello, A. Paulo, J.-L. Mergny, G.F. Salgado, J. A. Queiroz, C. Cruz, Aptamer-based targeted delivery of a G-quadruplex ligand in cervical cancer cells, Sci. Rep. 9 (2019) 1–12.
[40] H. Sun, X. Zhu, P.Y. Lu, R.R. Rosato, W. Tan, Y. Zu, Oligonucleotide aptamers: new tools for targeted cancer therapy, Mol. Ther. Nucleic Acids 3 (2014) e182.
[41] J. Wu, C. Song, C. Jiang, X. Shen, Q. Qiao, Y. Hu, Nucleolin targeting AS1411 modified protein nanoparticle for antitumor drugs delivery, Mol. Pharm. 10 (2013) 3555–3563.
[42] C. Riccardi, C. Fàbrega, S. Grijalvo, G. Vitiello, G. D'Errico, R. Eritja, D. Montesarchio, AS1411-decorated niosomes as effective nanocarriers for Ru (iii)-based drugs in anticancer strategies, J. Mater. Chem. B 6 (2018) 5368–5384.
[43] M. Alibolandi, S.M. Taghdisi, P. Ramezani, F.H. Shamili, S.A. Farzad, K. Abnous, M. Ramezani, Smart AS1411-aptamer conjugated pegylated PAMAM dendrimer for the superior delivery of camptothecin to colon adenocarcinoma in vitro and in vivo, Int. J. Pharm. 519 (2017) 352–364.
[44] M. Alibolandi, M. Ramezani, K. Abnous, F. Hadizadeh, AS1411 aptamer-decorated biodegradable polyethylene glycol–poly (lactic-co-glycolic acid) nanopolymersomes for the targeted delivery of gemcitabine to non–small cell lung cancer in vitro, J. Pharm. Sci. 105 (2016) 1741–1750.
[45] M.T. de Pinho Favaro, U. Unzueta, M. de Cabo, A. Villaverde, N. Ferrer-Miralles, A. R. Azzoni, Intracellular trafficking of a dynein-based nanoparticle designed for gene delivery, Eur. J. Pharm. Sci. 112 (2018) 71–78.
[46] M. Bogacheva, A. Egorova, A. Slita, M. Maretina, V. Baranov, A. Kiselev, Arginine-rich cross-linking peptides with different SV40 nuclear localization signal content as vectors for intranuclear DNA delivery, Bioorg. Med. Chem. Lett. 27 (2017) 4781–4785.